Finding Brown Dwarfs Within The COSMOS survey

Alasdair Koplick (10729216)
Project partner: Ewan Scopes
(Dated: December 31, 2023)

We obtained three lists of brown dwarfs from the COSMOS survey using data from the VISTA and SUBARU telescopes. The selection process eliminated galaxies from the catalogue by removing objects too wide to be a point source, too faint in the J-Band, and outside of the stellar locus in the H - Ks, Y - J colour-colour space. The LOWZ and Sonora Bobcat brown dwarf model sets were tested and determined to be suitable for this project and used to eliminate non brown dwarf sources. This was done by fitting the model spectra to the spectra of the COSMOS survey and removing any fits with a reduced χ^2 above a threshold. An extra was also performed check by only taking spectra that were better fit by the brown dwarf models than a series of galaxy models. The three lists of brown dwarfs found were those fitted with the LOWZ models (1723 sources), the Sonora Bobcat models (1776 sources), and the list of overlap between the two (1580 sources). These lists should help future analysis of parameters of brown dwarf populations, such as the scale height.

INTRODUCTION

Brown dwarfs are a family of objects first theorised in 1962 by S. S. Kumar[1] and with the first confirmed brown dwarf (Tiede 1) being published in 1995[2]. The key distinction from other stellar families is their inability to fuse hydrogen, placing a maximum limit on their mass at the hydrogen burning limit, around $0.064M_\odot - 0.087M_\odot$[3] or $\approx 67M_J - 91M_J$ (where M_J denotes Jupiter masses). The current smallest brown dwarfs were found with the JWST NIRCam with a mass of $3 - 4M_J$[4]. As hydrogen fusion never ignites during the formation process of brown dwarfs, gravity forces the electrons into a degenerate gas, and hence the weight of the star is supported through electron degeneracy pressure, leading to an object that doesn't produce its own heat but instead slowly cools. A model of brown dwarf interiors based on non-relativistic electron degeneracy was first produced by S. S. Kumar in 1963[3][5]. Brown dwarf radii range from $0.64R_J - 1.13R_J$[6] and Brown dwarfs occupy spectral types M, L and T, with a maximum effective temperature (T_{ef}) of $2930K$ reached for the M5.5 spectral type[7]. A set of example spectra define the features of each spectral type, as set out in the SpeX standards library[8], shown in Fig 1. In total brown dwarfs account for roughly 50% of the stars in our local neighbourhood in the Milky way[9].

A key property of brown dwarfs is their very long lifetimes, slowly cooling until no longer visible, instead of having a life limited by hydrogen reserves like a main sequence star. This makes them useful objects for providing information about the structure of the Milky way, for example, comparing the scale heights of populations of brown dwarfs with different metallicities or spectral types can tell us how orbits in the Milky way and hence its structure evolves over long periods of time. Of more concern, they predominantly emit in the near infrared (NIR) region, making them a large contaminant population for projects aiming to look out of our galaxy at

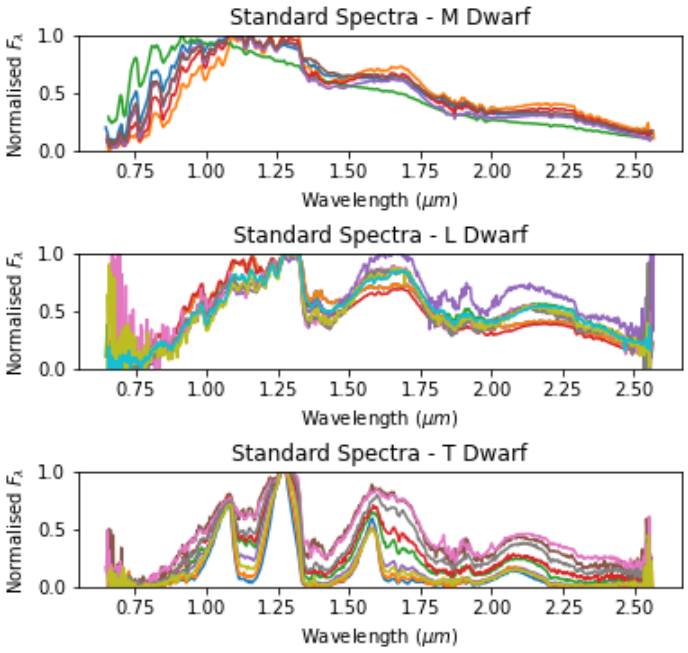

FIG. 1: Plotted spectra for brown dwarfs of M,L and T spectral types from the SpeX library. There are no SpeX spectra for spectral type Y brown dwarfs.

these frequencies[9]. Their spectra also closely mimics that of redshift z = 6 galaxies (as demonstrated in Fig 2). This makes information about the scale heights of brown dwarf populations important so they can be removed from datasets to prevent mis-identification of objects in projects looking at high redshift galaxys, such as the Euclid Satellite[10]. Conversely this property also makes it challenging to locate brown dwarfs in existing datasets to study their scale height.

Several papers have previously looked at identifying brown dwarfs within datasets and estimating their scale height, however it is still not well known, with the latest

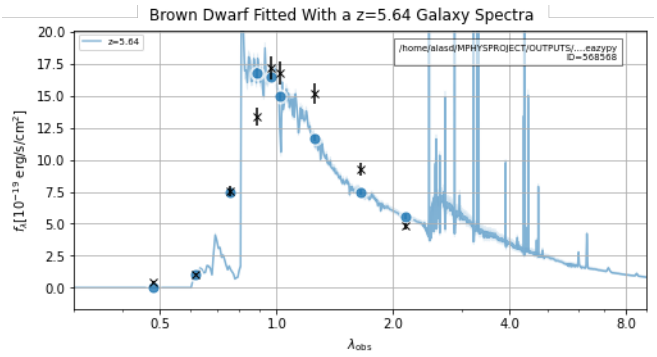

FIG. 2: Spectra of a z=5.64 galaxy (blue) overlayed with filter integrated spectra of a brown dwarf (black). Similarities in the shapes of both can be seen.

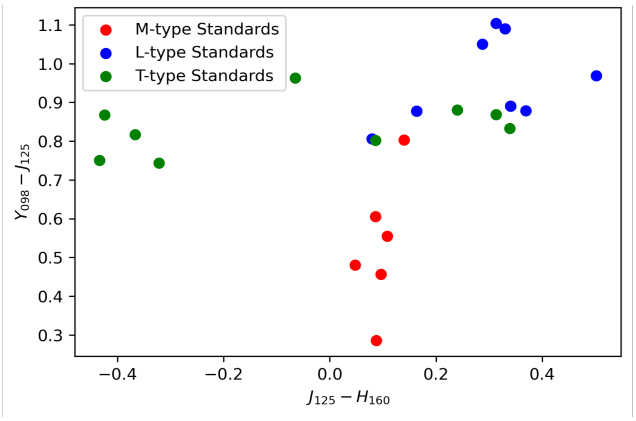

FIG. 3: Y-J vs J-H band colour-colour plot of the SpeX standards. Previous papers such as Ryan have used this plot to select brown dwarfs by drawing boxes within it.

value being $290 \pm 20pc$ from van Vledder et al. (2016), and with older papers suggesting values from $\approx 250pc$ (Jurić et al. 2008) up to $400 \pm 100pc$ (Holwerda et al. 2014)[11]. Previous papers such as Aganze et al. (2022)[9] or Ryan et al. (2011)[12] have also had limited datasets compared to the COSMOS survey[13] we are using in this project, being focused on brown dwarfs either within our galactic neighbourhood or very far from it respectively. These papers have also used different methods to find brown dwarfs within datasets, such as the combination of spectral line features, random forest classifers and deep neural networks in Aganze et al. (2022)[9], or by plotting differences in flux bands against each other (colour-colour space method) and drawing a box within these plots to select objects in Ryan et al.(2011)[12], see Fig 3. Notably, our method significantly improves on the second of these as we have access to the Ks flux band, which is especially useful for isolating stars from galaxies, see Fig 4. This results in two distinct groups for the stars and galaxies allowing us to fit and remove the galaxies with a straight line, instead of drawing boxes within the entire

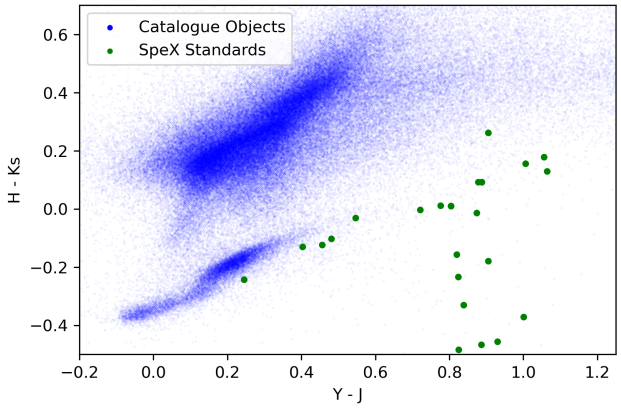

FIG. 4: Y-J vs H-Ks band colour-colour plot of the COSMOS catalogue and the SpeX standards. Using the Ks band, the colour-colour space seperates stars and galaxies into two distinct groups (bottom and top respectively) either side of a straight line, allowing a more precise removal of galaxies.

colour-colour space. This is similar to analysis done by M Jarvis at al. in 2012[14].

In this report, we analyse several sets of brown dwarf model spectra across different effective temperatures and metalicites, such as the Bobcat Sonora models[15] and the LOWZ models[16]. Firstly ensuring that they properly cover the range of brown dwarf spectral types we expect in colour-colour space, and secondly that they fit the spectra of a set of known brown dwarfs well. Once confident with our model selection we then trim the catalogue to only include brown dwarfs using flux radius of sources, their J-band magnitude and by fitting the stellar locus in H - Ks, Y - J colour-colour space. Finally we use the eazpy python library to compare our trimmed catalogue spectra to both our model spectra and a set of galaxy spectra. This allowed the selection of sources where both the brown dwarf models fit better than the galaxy models and where the dwarf models fit with a reduced χ^2 better than a determined cutoff. A third set of brown dwarfs was obtained from the overlap between the LOWZ and Sonora Bobcat models.

THEORY

As outlined in the previous section, brown dwarfs have mass range of $\approx 4M_J - 75M_J$[3][4] and a radius range of $0.64R_J - 1.13R_J$[6]. Calculating the acceleration due to gravity for these ranges with;

$$g = \frac{GM_{dwarf}}{R^2} \tag{1}$$

we find the logarithm of the acceleration for all brown dwarfs $\log g \approx 5$ in CGS units (referred to as surface gravity), a parameter used to characterise the model brown

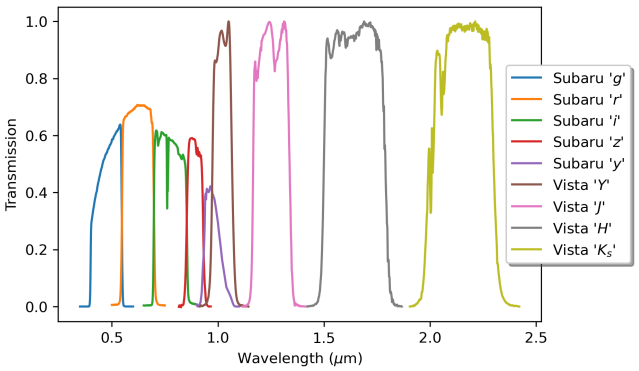

FIG. 5: Filter Response curves for the nine filters selected from the Subaru and VISTA telescopes.

dwarf spectra. Another key parameter is the effective temperature, T_{ef}. For a given star its T_eff is the temperature a blackbody would have to be at to emit the same amount of power (through EM radiation). We can therefore use the Stefan Boltzman law and equate to the luminosity per surface area to define the relation:

$$\frac{L}{4\pi R^2} = F_{bol} = \sigma T^4 \tag{2}$$

where L is the total luminosity of the star, and F_{bol} is bolometric flux, the flux emitted per unit area of the star.

To look at the relevant frequencies of the COSMOS survey (or catalogue), the bandpass filters Y, J, H and Ks from the VISTA telescope[17] and g, r, i, z and y from the Subaru telescope[18] were selected. This ensured good coverage from $0.4\mu m$ to $2.5\mu m$, the wavelengths where brown dwarf spectra are most prominent. This is shown in Fig 5, where the filter response curves demonstrate how the intensity of a flat spectra would look through these filters. All fluxes were converted into frequency dependant flux f_ν from wavelength dependant flux f_λ using Equation 3:

$$f_\nu = f_\lambda \frac{\lambda^2}{c}, \tag{3}$$

from

$$\nu = \frac{c}{\lambda} \tag{4}$$

to keep everything similar. All magnitudes were also converted into AB or "absolute brightness" magnitudes, a magnitude system a with zero magnitude corresponding to 3631 Janskys, as opposed to an astronomical source. This gives a conversion of:

$$m_{AB} = -2.5 \log_{10} \frac{f_\nu}{3631} \tag{5}$$

from f_ν.

To produce plots in colour-colour space, the spectra from each source is convolved with the filter response of each band. This produces nine fluxes for each source, one for every filter band. This is shown below in Equation 6:

$$f_{conv} = \frac{\int R_\nu f_\nu \, d\nu}{\int R_\nu \, d\nu} \tag{6}$$

but since the spectra are discrete, this becomes:

$$f_{conv} = \frac{\sum R_i f_i}{\sum R_i} \tag{7}$$

where R_i is the ith point of the filter response curve, and f_i the corresponding point of the flux of the spectra. This also required interpolation to ensure the ith flux and filter response points were at the same wavelength. To prevent aliasing, interpolation was done between the spectra points then matched to the wavelength positions of the filter response, as the spectra points were more closely spaced. The convolved flux from each filter band or "colour" can then be converted to an AB magnitude, and differences in magnitude between colours can be plotted for each spectra, giving Fig 3 for the SpeX standard spectra.

METHOD

The spectra fitting routine at the end of the selection process requires a set of model brown dwarf spectra. To find the most suitable, three model sets were tested against both the SpeX standards and a list of 9 objects from the COSMOS survey confirmed to be brown dwarfs by Aganze et al. (2022)[9] (referred to as confirmed dwarfs). The Galaxies were then removed from the catalogue, leaving only a set of stars. This was then trimmed to only contain brown dwarfs using the eazypy python library[19] and the model sets selected earlier, finally T_{ef} and type of each source could be estimated. Errors on T_{ef} were then calculated.

Model Selection

Each set of models consists of a set of spectra modelled at varying T_{ef}, metallicity and surface gravity. The Sonora Bobcat[15], LOWZ[16] and ATMOS model[20] sets were chosen. Initially we selected the models with a surface gravity of $\log_{10} g = 5$ to speed up the model selection process, as this is the rough value for a brown dwarf (see previous section). This constraint was later removed when fitting COSMOS catalogue for our final brown dwarf selection. These models were then smoothed to the same resolution as the SpeX standards, to remove fine emission line details that would not be observable by a telescope. This helped the model spectra better match the observed spectra from the COSMOS survey. The model sets were first tested by visual inspection against

the SpeX standards. The standards and models were plotted in Y-J J-H colour-colour space, with the models being checked to see if they properly covered the SpeX standards. From this it was concluded that the ATMOS models were not suitable as they did not overlap the standards anywhere, and where ATMOS and the standards were close there were relatively few models. The LOWZ and Bobcat model sets were kept and then tested against the confirmed dwarfs using the eazypy python library[19] to fit the model spectra to the confirmed dwarf spectra. Table I shows the reduced χ^2 of the best fitting model spectra from Bobcat and LOWZ to each Confirmed Dwarf. Although the χ^2s in Table I vary by a

TABLE I: Reduced χ^2 For LOWZ And Bobcat Model Sets Fitted To Confirmed Dwarfs

Dwarf ID	Bobcat Reduced χ^2	LOWZ Reduced χ^2
568568	0.521	9.659
624866	0.586	0.773
482712	0.241	32.866
692895	0.360	0.602
609792	2.409	2.967
590761	25.682	25.682
549461	22.850	22.850
607359	0.753	0.859
547131	1.421	8.774

significant amount, since both models produced a similar range of χ^2 values, both were kept. The two identical values for dwarfs 590761 and 549461 are discussed later in Section .

Removing Galaxies

Galaxies were then removed in a similar process to the analysis performed by M Jarvis et al. (2012)[14], the entire COSMOS catalogue was plotted in Y-J vs H-Ks colour-colour space along with the SpeX standards and the confirmed dwarfs. As shown in Fig 4, this separates the stars and galaxies into the bottom and top groupings respectively. The stellar locus (bottom group) is then fitted with a straight line through the highest density region. The graph is also flattened for easier visualisation. The density of COSMOS catalogue sources is then sampled along horizontal lines above the stellar locus fit until it drops to half the original value. The full width at half maximum (FWHM) can then be found by doubling this value, since we have only found the distance from the peak of the distribution to one side of the FWHM. Assuming distribution of points is Gaussian, the FWHM

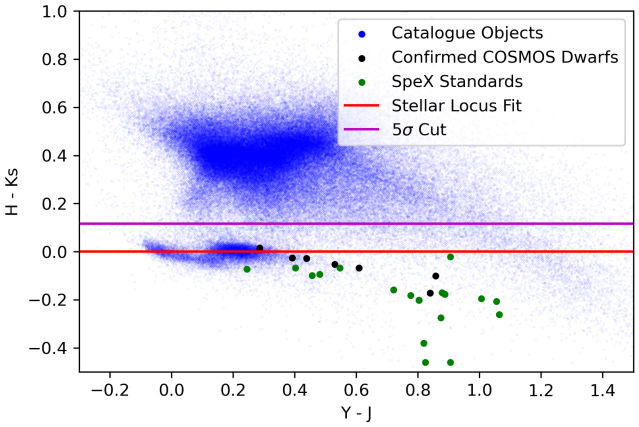

FIG. 6: Y-J vs H-Ks band colour-colour plot of the COSMOS catalogue, SpeX standards and confirmed dwarfs. The red and purple lines are the fit to the Stellar Locus and the 5σ distance from the stellar locus distribution respectively.

can be related the to standard deviation σ as:

$$\sigma = \frac{FWHM}{2\sqrt{2\ln 2}} \approx \frac{FWHM}{2.355} \tag{8}$$

This allows us to remove any sources outside 5σ from the centre of the stellar locus distribution. This trimmed the COSMOS catalogue down from $\sim 930,000$ to $\sim 85,000$, removing over 90% of all sources.

Isolating Brown Dwarfs

Non brown dwarf sources were now removed. We used the eazypy python library by Gabe Brammer[19] to fit the LOWZ and Sonora Bobcat model spectra to the filter convolved spectra of each source in our catalogue. This fitted every spectra from the model set and then found the one with the lowest χ^2. The catalogue was also run against a set of galaxy spectra that were tested at different redshifts. This gave a second check on galaxies as sources where $\chi^2_{GAL} < \chi^2_{STAR}$ could be discarded. To determine which sources were brown dwarfs rather than stars, the maximum reduced χ^2 from the confirmed dwarfs was taken as a hard cuttoff (seen in Table I), so for the LOWZ spectra fits sources with a reduced χ^2 higher than 33 were removed. This produced two lists of brown dwarfs, one fitted with the LOWZ models and one fitted with the Sonora Bobcat models. Additionally a third list containing the common sources between the two was produced, this should hopefully reduce outliers from the weaknesses of the different models as discussed in Section .

Obtaining Effective Temperature, Type and Distance

From eazypy the best fitting spectra of the model set is obtained for each source. The parameters that the spectra has been modeled at then provide best estimates on T_{ef}, metallicity and surface gravity of that source. T_{ef} can then be compared to a conversion table to spectral type, such as from E Mamajek (2022)[7]. Since the listed temperatures from E Mamajek (2022) and the model T_{ef} were not identical, T_{ef} was matched to the closest spectral type, providing error to ± 1 at the most on the spectral type selection.

Distances for could then be calculated using Table 3 from J Caballero et al. (2018)[21]. This provides absolute magnitudes in the J band for several brown dwarf types, allowing us to use:

$$m - M = -5 + 5 \log d \tag{9}$$

where m is the apparent magnitude in the J band observed by COSMOS, and d is the distance in parsecs. As some spectral types were not given by J Caballero et al. (2018), distances could only be calculated for some of the sources (those that couldn't are marked as N/A in the final lists).

Error Calculation for Effective Temperature

To find errors on T_{ef}, the reduced χ^2 of the every model spectra at different T_{ef} was considered. The set of models should form a parabola in T_{ef}, χ^2 space, with the minimum χ^2 being the best fitting model. This allows a $\chi^2 + 1$ line to be drawn and the error taken from the intersection of the line and parabola. This is show in Fig 7. Several edge cases were encountered, such as the minimum existing at the very edge of the T_{ef} axis and hence only intersecting the $\chi^2 + 1$ line once. In this case the existing intersection was mirrored. In other cases the entirety of the parabola existed between the χ^2 and the $\chi^2 + 1$ lines. Here the entire range of T_{ef} for the model set was taken as the error. These edge cases are discussed further in Section .

RESULTS

For the three lists produced

Model Investigation

talk about temperature range etc...

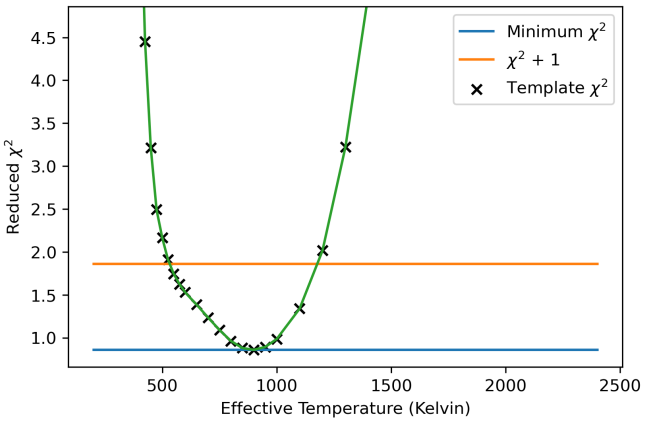

FIG. 7

Sample from COSMOS

DISCUSSION AND FURTHER THING

using cholla models worse error on Tef for dimmer spectral types, both dimmer so more error and more poorly understood so worse models.

Misidentification of Dwarfs in the Confirmed Set

Linear Interpolation and Ks Space Stellar Locus Cut (and tail in fig 6)

ACKNOWLEDGEMENTS

This research has benefited from the SpeX Prism Spectral Libraries, maintained by Adam Burgasser at http://www.browndwarfs.org/spexprism.

I'd also like to thank my project partner Ewan Scopes and supervisor Rebecca Bowler, for all the assistance as well as patience they've had for me and my problems.

[1] S. S. Kumar, Study of Degeneracy in Very Light Stars., **67**, 579 (1962).
[2] R. Rebolo, M. R. Zapatero Osorio, and E. L. Martín, Discovery of a brown dwarf in the Pleiades star cluster, Nature (London) **377**, 129 (1995).
[3] S. Auddy, S. Basu, and S. R. Valluri, Analytic models of brown dwarfs and the substellar mass limit, Advances in Astronomy **2016**, 1–15 (2016).
[4] K. L. Luhman, C. A. de Oliveira, I. Baraffe, G. Chabrier, T. R. Geballe, R. J. Parker, Y. J. Pendleton, and P. Tremblin, A jwst survey for planetary mass brown dwarfs in ic 348*, The Astronomical Journal **167**, 19 (2023).

TABLE II: Selection Of Identified Brown Dwarfs From The Overlap List

COSMOS ID	Effective Temperature T_{ef} (K)	Uncertainty $\sigma_{T_{ef}}$	Dwarf Type	Distance
6394	2400	19	M8.5V	0.716
7236	2400	22	M8.5V	0.212
9836	1600	60	L6V	0.154
73432	2200	162	L1V	0.93
162238	1000	113	T5.5V	0.785
435353	950	319	T6V	0.664
550804	400	128	Y0.5V	N/A
764732	275	107	Y4V	N/A

[5] S. S. Kumar, The Helmholtz-Kelvin Time Scale for Stars of Very Low Mass., Astrophys. J. **137**, 1126 (1963).

[6] S. Sorahana, I. Yamamura, and H. Murakami, On the Radii of Brown Dwarfs Measured with AKARI Near-infrared Spectroscopy, Astrophys. J. **767**, 77 (2013), arXiv:1304.1259 [astro-ph.SR].

[7] E. Mamajek, A modern mean dwarf stellar color and effective temperature sequence, `http://www.pas.rochester.edu/~emamajek/EEM_dwarf_UBVIJHK_colors_Teff.txt` (2022), accessed: 20.12.23.

[8] Http://www.browndwarfs.org/spexprism.

[9] C. Aganze, A. J. Burgasser, M. Malkan, C. A. Theissen, R. A. Tejada Arevalo, C.-C. Hsu, D. C. Bardalez Gagliuffi, R. E. Ryan, and B. Holwerda, Beyond the Local Volume. I. Surface Densities of Ultracool Dwarfs in Deep HST/WFC3 Parallel Fields, Astrophys. J. **924**, 114 (2022), arXiv:2110.07672 [astro-ph.SR].

[10] G. D. Racca, R. Laureijs, L. Stagnaro, J.-C. Salvignol, J. Lorenzo Alvarez, G. Saavedra Criado, L. Gaspar Venancio, A. Short, P. Strada, T. Bönke, C. Colombo, A. Calvi, E. Maiorano, O. Piersanti, S. Prezelus, P. Rosato, J. Pinel, H. Rozemeijer, V. Lesna, P. Musi, M. Sias, A. Anselmi, V. Cazaubiel, L. Vaillon, Y. Mellier, J. Amiaux, M. Berthé, M. Sauvage, R. Azzollini, M. Cropper, S. Pottinger, K. Jahnke, A. Ealet, T. Maciaszek, F. Pasian, A. Zacchei, R. Scaramella, J. Hoar, R. Kohley, R. Vavrek, A. Rudolph, and M. Schmidt, The euclid mission design, in *Space Telescopes and Instrumentation 2016: Optical, Infrared, and Millimeter Wave*, edited by H. A. MacEwen, G. G. Fazio, M. Lystrup, N. Batalha, N. Siegler, and E. C. Tong (SPIE, 2016).

[11] R. E. Ryan, P. A. Thorman, S. J. Schmidt, S. H. Cohen, N. P. Hathi, B. W. Holwerda, J. I. Lunine, N. Pirzkal, R. A. Windhorst, and E. Young, The effect of atmospheric cooling on vertical velocity dispersion and density distribution of brown dwarfs, The Astrophysical Journal **847**, 53 (2017).

[12] R. E. Ryan, P. A. Thorman, H. Yan, X. Fan, L. Yan, M. R. Mechtley, N. P. Hathi, S. H. Cohen, R. A. Windhorst, P. J. McCarthy, and D. M. Wittman, Hubble Space Telescope Observations of Field Ultracool Dwarfs at High Galactic Latitude, Astrophys. J. **739**, 83 (2011), arXiv:1105.2567 [astro-ph.GA].

[13] J. R. Weaver, O. B. Kauffmann, O. Ilbert, H. J. McCracken, A. Moneti, S. Toft, G. Brammer, M. Shuntov, I. Davidzon, B. C. Hsieh, C. Laigle, A. Anastasiou, C. K. Jespersen, J. Vinther, P. Capak, C. M. Casey, C. J. R. McPartland, B. Milvang-Jensen, B. Mobasher, D. B. Sanders, L. Zalesky, S. Arnouts, H. Aussel, J. S. Dunlop, A. Faisst, M. Franx, L. J. Furtak, J. P. U. Fynbo, K. M. L. Gould, T. R. Greve, S. Gwyn, J. S. Kartaltepe, D. Kashino, A. M. Koekemoer, V. Kokorev, O. Le Fèvre, S. Lilly, D. Masters, G. Magdis, V. Mehta, Y. Peng, D. A. Riechers, M. Salvato, M. Sawicki, C. Scarlata, N. Scoville, R. Shirley, J. D. Silverman, A. Sneppen, V. Smolcić, C. Steinhardt, D. Stern, M. Tanaka, Y. Taniguchi, H. I. Teplitz, M. Vaccari, W. H. Wang, and G. Zamorani, COSMOS2020: A Panchromatic View of the Universe to z∼10 from Two Complementary Catalogs, **258**, 11 (2022), arXiv:2110.13923 [astro-ph.GA].

[14] M. J. Jarvis, D. G. Bonfield, V. A. Bruce, J. E. Geach, K. McAlpine, R. J. McLure, E. González-Solares, M. Irwin, J. Lewis, A. K. Yoldas, S. Andreon, N. J. G. Cross, J. P. Emerson, G. Dalton, J. S. Dunlop, S. T. Hodgkin, F. O. Le, M. Karouzos, K. Meisenheimer, S. Oliver, S. Rawlings, C. Simpson, I. Smail, D. J. B. Smith, M. Sullivan, W. Sutherland, S. V. White, and J. T. L. Zwart, The VISTA Deep Extragalactic Observations (VIDEO) survey, **428**, 1281 (2013), arXiv:1206.4263 [astro-ph.CO].

[15] M. S. Marley, D. Saumon, C. Visscher, R. Lupu, R. Freedman, C. Morley, J. J. Fortney, C. Seay, A. J. R. W. Smith, D. J. Teal, and R. Wang, The Sonora Brown Dwarf Atmosphere and Evolution Models. I. Model Description and Application to Cloudless Atmospheres in Rainout Chemical Equilibrium, Astrophys. J. **920**, 85 (2021), arXiv:2107.07434 [astro-ph.SR].

[16] A. M. Meisner *et al.*, New candidate extreme t subdwarfs from the backyard worlds: Planet 9 citizen science project, The Astrophysical Journal **915**, 120 (2021).

[17] W. Sutherland, J. Emerson, G. Dalton, E. Atad-Ettedgui, S. Beard, R. Bennett, N. Bezawada, A. Born, M. Caldwell, P. Clark, S. Craig, D. Henry, P. Jeffers, B. Little, A. McPherson, J. Murray, M. Stewart, B. Stobie, D. Terrett, K. Ward, M. Whalley, and G. Woodhouse, The visible and infrared survey telescope for astronomy (VISTA): Design, technical overview, and performance, Astronomy &amp Astrophysics **575**, A25 (2015).

[18] M. IYE, Subaru telescope —history, active/adaptive optics, instruments, and scientific achievements—, Proceedings of the Japan Academy, Series B **97**, 337 (2021).

[19] G. Brammer, eazy-py (2021).

[20] M. W. Phillips, P. Tremblin, I. Baraffe, G. Chabrier, N. F. Allard, F. Spiegelman, J. M. Goyal, B. Drummond, and E. Hébrard, A new set of atmosphere and evolution models for cool T-Y brown dwarfs and giant exoplanets, aap **637**, A38 (2020), arXiv:2003.13717 [astro-ph.SR].
[21] J. A. Caballero, A. J. Burgasser, and R. Klement, Contamination by field late-M, L, and T dwarfs in deep surveys, **488**, 181 (2008), arXiv:0805.4480 [astro-ph].